QUADRUPOLE IMAGE-CURRENT EFFECTS IN THE ITS 6-MeV, 4-kA LINAC

Paul Allison and David C. Moir
Los Alamos National Laboratory

Abstract

The eight accelerating cells for the ITS linear induction accelerator (LIA) are driven with two 50-Ω lines at 250 kV for 60 ns. The wall return currents for the 4-kA beam then pass through these lines, generating a weak steady-state quadrupole field of ~ 3 G integrated strength on axis, which causes a small asymmetry in the nominally round beam at the linac exit. Beam-dynamics simulations with the particle-tracing code SCHAR show that if uncorrected, this would increase the beam emittance at the end of the DARHT 20-MeV linac, therefore quadrupole-corrector coils (QC) were added to each cell, in addition to the existing dipole steering coils. Measurements of the asymmetry of the ITS beam as a function of excitation current of these corrector coils are in good agreement with simulations, giving confidence that there will be negligible emittance degradation from this effect for DARHT.

INTRODUCTION

The DARHT accelerator[1] is designed to produce a 20-MeV, 4-kA beam of 60-ns duration, focused to about 1-mm diam on a tungsten target for flash X-ray measurements of explosive shots. Focusing (by solenoids) and acceleration are axisymmetric, therefore the beam should always be round. However, in initial

Fig.1 Layout of ITS for quadrupole experiment

measurements on the ITS prototype (layout shown in Fig.1) we found significant asymmetries after acceleration through the first block of eight induction cells, particularly with weak focusing transport. The source of asymmetry is presumably a weak quadrupole image field (QIF) produced by wall return currents into the drive rods

of the accelerating cells (Fig.2). Calculations with the code SCHAR[2] showed that the QIF would have a negligible effect under the conditions of the design tune but might lead to significant emittance growth and beam asymmetry under other conditions.
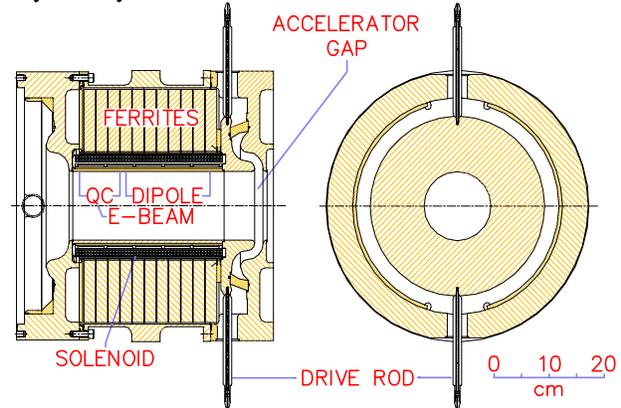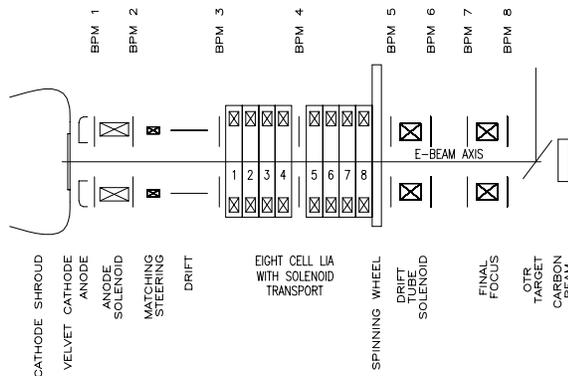

Fig.2 ITS accelerating cell geometry

Our cell uses two drive rods to supply cell voltage. This symmetry eliminates dipole fields produced by the drive rods, which each carry $(i_b + i_f)/2$, where $i_b = 4$ kA and ferrite current $i_f = 500$ A, both approximately constant during the 60-ns pulse. We designed[3] the cell for minimum transverse impedance and discovered during RF measurements[4] of prototypes that the normally degenerate TM_{110}-like modes were split by ~ 100 MHz by the rods coupling into the drive lines, reducing the frequency-averaged impedance by about half. Four drive rods would eliminate the QIF but at the cost of higher transverse impedance.

The integrated strength $b \equiv \int g dz$, with $g \equiv \nabla_\perp B$, of the QIF can be estimated[5] by assuming that the wall current i_b crosses the gap w = 1.9 cm, half at $0°$ and half at $180°$, at distance D = 23.3 cm from the axis, leading to $b \sim i_b Z_o w / 2\pi c D^2 = 0.70$ G/kA. Calculations[5] with the 3-D code BTEC, using ferrite permeability 250, give b = 1.0 G/kA, or 0.77 G/kA without the ferrites. Each cell already had a Lambertson-type dipole steering pair for beam alignment, so we added a quadrupole corrector (QC) circuit to the printed-circuit foil. Since the quadrupole strength depends only on beam current, which is constant through the linac, a single power supply of ~ 3 A can be used to null the QIF.

The single-particle dynamics for continuous solenoidal field B and quadrupole gradient g for a beam without acceleration give $x'' = ky' + Gx$ and $y'' = -(kx' + gy)$, where $k = B/B\rho$ and $G = g/B\rho$. Combining these leads to $y'''' + k^2 y'' - G^2 y = 0$ and

similarly in x, the solution to which is $\exp(i\Omega z)$, where $\Omega^2 = k^2 \pm (k^2 + 4G^2)^{1/2}$. Thus, there is exponential growth unless $G \equiv 0$. With $g \sim 3$ G/43cm and $B \sim 2$ kG, $\Omega \sim \pm 1/20$ cm, $\pm i/286$ m. The accelerator length L for DARHT is 32.2 m, making the exponential growth factor only ~ 1.1. Emittance calculated with SCHAR grows very rapidly with quadrupole strength but is low at the nominal strength, in qualitative agreement with this simple model. The QIF changes the beam angle r' by $\delta r' \sim br/B\rho$ per cell, which should be made small compared with the thermal spread $\theta \sim \varepsilon_n/\beta\gamma r$, leading to beam radius $r \ll (mc\varepsilon_n/eb)^{1/2} = 7$ cm for 4rms normalized emittance $\varepsilon_n = 0.14\pi$-cm-rad. For DARHT, r varies from about 1 cm at injection to 0.5 cm at the exit, well under 7 cm.

EXPERIMENT

For this experiment, the QC were added to cells #5-8 only. The QC location (Fig.2) is close to the accelerating gap but displaced by one cell, hence in operation the first QC in DARHT will probably not be used. A field map of the QC in the cell showed that its strength was increased $\sim 60\%$ over the air value to 1.1 G/A. We operated all eight linac solenoids at 140 A, about 500 G peak and less than half the design value, to make the beam radius larger to enhance the QIF effect. All four QC's were operated in series over the their maximum range, ± 20 A. The injector was operated at 3.55 MeV, 3 kA, and the accelerating cells were operated at 214 kV each, giving 5.26 MeV final energy.

A line schematic of the experimental set-up for optical measurement of ellipticity is shown in Fig.3. The electron beam is focussed on a 6-μm-thick aluminized Kapton (Al/K) detector that is located 64.2 cm from the center of the final focus magnet. The beam interacts with the foil to produce optical transition radiation (OTR). This visible light is imaged on the photocathode of a gated microchannel plate (MCP). The MCP is gated for 20 ns and timed to be in the center of the 60-ns flat-top of the beam pulse. A cooled ccd camera interfaced to the MCP is used to collect the image data. The rms beam diameter was typically 15 mm. The targets were not damaged for
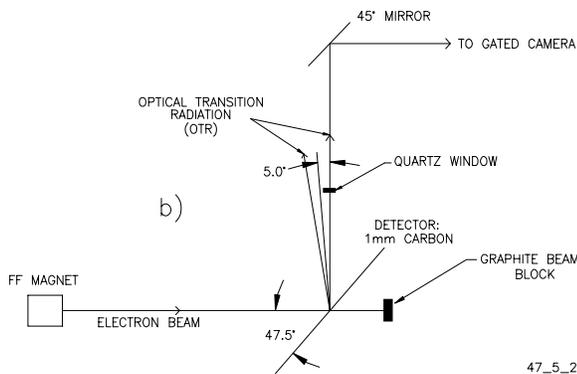
Fig.3 Schematic of OTR measurement

these beam parameters. All of the data were taken with the same micro-channel plate gain and on the same Al/K surface. As a result this data is internally consistent.

Contour plots of the electron beam distribution inferred from OTR measurements as a function of quadrupole magnet current are shown in Fig.4. The inner, intermediate and outer contours correspond to 10%, 40% and 80% of the peak intensity**.** Beam distribution data at each of the quadrupole currents is analyzed to obtained the rms radius and then the image is rotated 15° and reanalyzed to obtain the rms radius. This process is continued through 165°. The result is the rms radius vs angle for a single beam-pulse distribution. The ratio of minimum to maximum of this rms radius vs angle is the experimental ellipticity, obtained for each QC setting, plotted in Fig.5.

Fig.5 Variation of ellipticity with quad corrector current
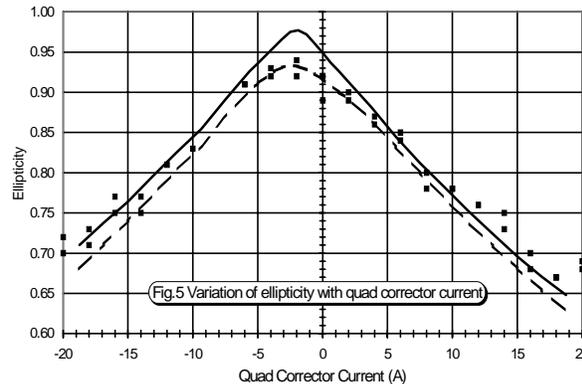
The SCHAR ellipticity at the target (solid curve, Fig.5) is slightly higher than the minimum (dashed curve) a few cm before the target. In SCHAR we used a calibration for QC of 89% of the measured and for QIF of 0.77 G/kA, 75% of the BTEC-calculated value with ferrites. Possibly the properties of the ferrites change in the presence of the solenoidal focusing field, or on the 60-ns time scale the values are different from those assumed. In spite of these differences, the measurements seem well explained by SCHAR.

CONCLUSIONS

We have shown that SCHAR predictions adequately match the measured ellipticity of the beam in ITS as a function of quadrupole corrector current. For the 4-kA matched tune for DARHT, SCHAR predicts ellipticity at the target of ~ 0.97 without using the QC and 0.99 with. Emittance growth is $< 4\%$ in either case. For beams mismatched by 50% at the linac entrance, ellipticity decreases to ~ 0.90 without and 0.96 with the QC. Calculated emittance growth is then about 6-12%, independent of either the QIF or QC. The dominant predicted quadrupole effect is therefore a barely observable ellipticity.

REFERENCES

[1] M. Burns, P. Allison, R. Carlson, J. Downing, D. Moir, and R. Shurter, "Status of DARHT", XVIII International Linac Conference, Geneva, August, 1996

[2] R. J. Hayden and M. J Jakobson, "The Space Charge Computer Program SCHAR", IEEE Trans. Nucl. Sci., Vol. NS-30, No. 4, August, 1983, p. 2540-2542. SCHAR traces distributions of line currents through an accelerator in steady state to all orders, using 3-D field maps of the accelerator and the self-fields of typically 1000 particles. Emittance growth can occur because of charge redistribution, field aberrations, energy spread across the beam, or the mixing of quadrupoles and solenoids in a transport.

[3] M. Burns, P. Allison, L. Earley, D. Liska, C. Mockler, J. Ruhe, H. Tucker, L. Walling, "Cell design for the DARHT linear induction accelerators", 1991 PAC, San Francisco

[4] L. Walling, Paul Allison, M. Burns, D. J. Liska, D. E. McMurry, "Transverse impedance measurements of prototype cavities for a dual-axis radiographic hydrotest facility", 1991 PAC, San Francisco

[5] Thomas P. Hughes, Robert E. Clark, Paul W. Allison, David C. Moir, "Multipole Field Calculations for DARHT", Beams 94 Conference
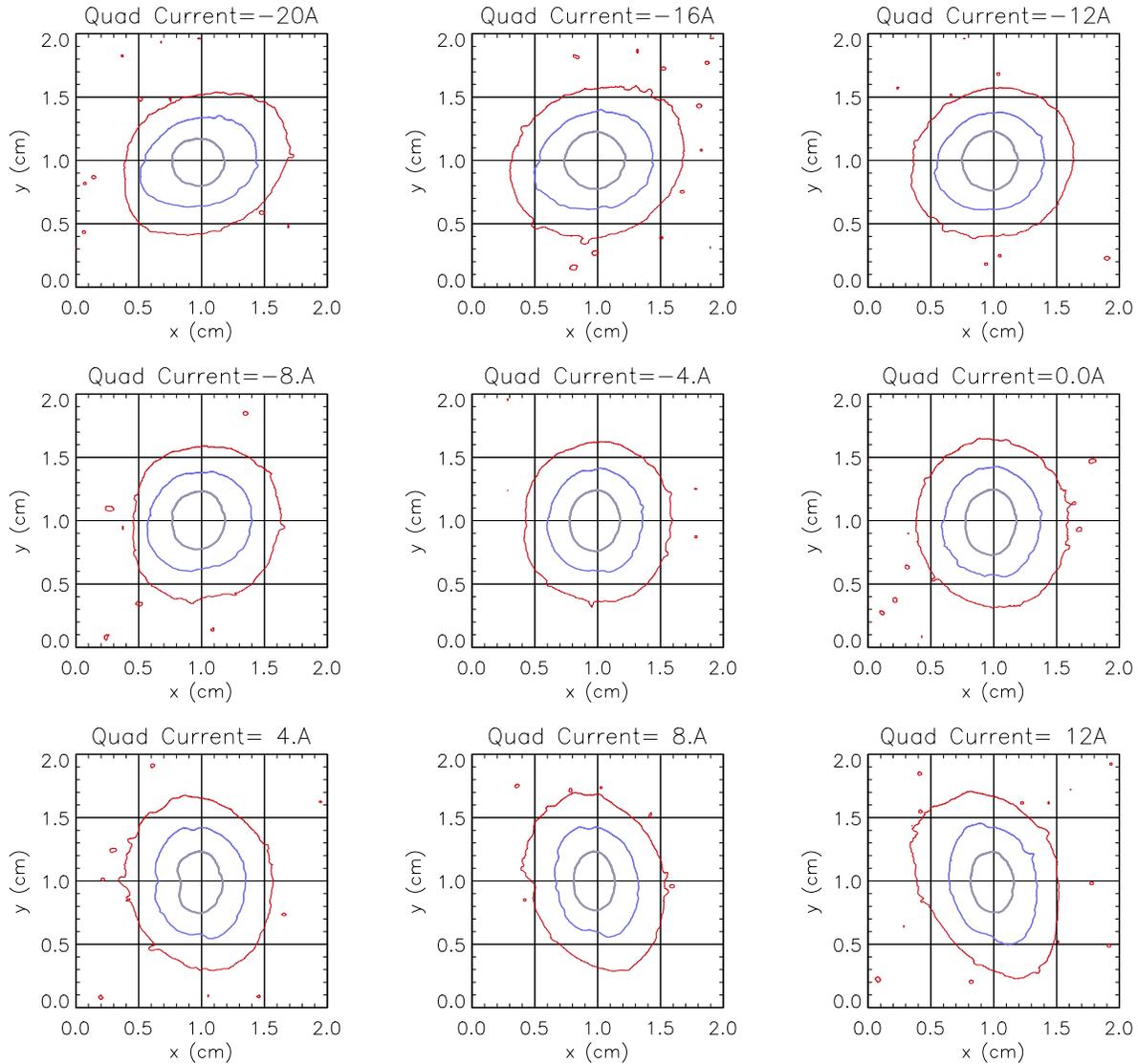
Fig.4 X- and Y-plane beam contours at OTR target vs QC current